Detecting long-term changes in point source fossil CO_2 emissions with tree ring archives

E. D. Keller[1], J. C. Turnbull[1,2] and M. W. Norris[1]

[1]{National Isotope Centre, GNS Science, Lower Hutt, New Zealand}

[2]{CIRES, University of Colorado at Boulder, CO, USA}

Correspondence to: E. D. Keller (l.keller@gns.cri.nz)

Abstract

We examine the utility of tree ring ^{14}C archives for detecting long term changes in fossil CO_2 emissions from a point source. Trees assimilate carbon from the atmosphere during photosynthesis, in the process faithfully recording the average atmospheric ^{14}C content in each new annual tree ring. Using ^{14}C as a proxy for fossil CO_2, we examine interannual variability over six years of fossil CO_2 observations between 2004-05 and 2011-12 from two trees growing near the Kapuni Natural Gas Plant in rural Taranaki, New Zealand. We quantify the amount of variability that can be attributed to transport and meteorology by simulating constant point source fossil CO_2 emissions over the observation period with the atmospheric transport model WindTrax. We compare model simulation results to observations and calculate the amount of change in emissions that we can detect with new observations over annual or multi-year time periods given both measurement uncertainty of 1ppm and the modelled variation in transport. In particular, we ask, what is the minimum amount of change in emissions that we can detect using this method, given a reference period of six years? We find that changes of 42% or more could be detected in a new sample from one year at the same observation location, or 22% in the case of four years of new samples. This threshold is reduced and the method becomes more practical the more the size of the signal increases. For point sources 10 times larger than the Kapuni plant (a more typical size for power plants worldwide), it would be possible to detect sustained emissions changes on the order of 10% given suitable meteorology and observations.

1   Introduction

Carbon dioxide (CO_2) emitted by anthropogenic activity is the largest single contributor to the radiative forcing causing climate change (IPCC, 2014). It thus plays a crucial role in any attempt to prevent or mitigate further warming. Large point sources (mainly from electricity generation and industry) contribute around a third of the total fossil-fuel derived CO_2 (CO_2ff) emissions (IPCC, 2014) and in many places are included in government regulatory schemes that aim to reduce emissions (e.g. European Union ETS, South Korea, Switzerland, and others at the city/state level; Serre et al., 2015). Emissions are typically reported on an annual basis, and commonly agreed-upon reduction targets are annual or multi-year caps, often requiring changes in emissions relative to a baseline year (e.g. the Kyoto Protocol and the new Intended Nationally Determined Contributions (INDC), UNFCCC, 2015).

Emissions are currently known from "bottom up" techniques such as self-reported data from fuel usage statistics (Boden et al., 2015) and/or continuous stack monitoring (U.S. Environmental Protection Agency, 2005; eGRID, 2014) and are subject to significant uncertainties (Ackerman and Sundquist, 2008; Gurney et al., 2009, 2012). This uncertainty might include not only methodological biases and possible deliberate underreporting but also simple error in compiling statistics. The integrity of regulation schemes and their effectiveness at limiting future climate change will require independent methods of evaluating reported emissions and improvement in the accuracy of emissions inventories (Tans and Wallace, 1999; Nisbet and Weiss, 2010; National Research Council, 2010; Gurney, 2013).

"Top-down" atmospheric observations can provide an independent method for evaluating emissions. This involves taking observations of atmospheric gas mole fractions in combination with atmospheric transport modelling to infer the magnitude of emissions from a source or region over a particular time period (e.g. McKain et al., 2012; Lindenmaier et al., 2014; Brioude et al., 2013). It can be quite challenging to quantify absolute values of emissions and CO_2 fluxes in general because of the large errors and biases typically encountered in transport models (e.g. Stephens et al., 2007; Lin and Gerbig, 2005; Gerbig et al., 2008; Prather et al., 2008; Geels et al., 2007; Liu et al., 2011; Kretschmer et al., 2012). However, *relative* changes in emissions are usually easier to determine, since any consistent biases in the model will cancel out. By establishing a baseline measurement over a reference period, we can compare future observations to this reference and calculate relative changes

1   that occur. In this manner, we can potentially verify relative emission reduction targets

2   without requiring precise knowledge of the absolute levels of emissions.

3   One of the biggest challenges of atmospheric observations of CO_2ff is distinguishing the

4   fossil component from the considerable background level of CO_2 that occurs naturally in the

5   atmosphere, currently about 400 parts per million (ppm; Mauna Loa observation record,

6   http://www.esrl.noaa.gov/gmd/ccgg/trends/index.html, last access: 13 May 2015). In addition,

7   there are large diurnally and seasonally varying CO_2 fluxes from the biosphere, which may

8   result in changes in CO_2 mole fraction of tens of ppm within a single day at near-surface sites

9   (e.g. Miles et al., 2012). This problem can be avoided by using the ^{14}C isotopic content as a

10 tracer for CO_2ff. CO_2ff contains no ^{14}C: the half-life of ^{14}C is 5,730 years (Karlen et al.,

11 1968), and all of the ^{14}C has decayed away from fossil fuels. Other sources of CO_2 have

12 roughly the same ^{14}C content as the atmosphere. By measuring the ^{14}C content of CO_2 or a

13 proxy for CO_2, we can calculate the portion of observed CO_2 that comes from recently added

14 fossil fuel emissions (Levin et al., 2003; Meijer et al., 1996; Turnbull et al., 2006).

15 Plant material can be used as a proxy for atmospheric CO_2ff because plants assimilate carbon

16 from the atmosphere during photosynthesis, in the process faithfully recording the ^{14}C content

17 in new plant material. Tree rings represent an integrated average of daytime CO_2 atmospheric

18 mole fractions and ^{14}C content over the tree's annual growth period, and can be independently

19 dated using dendrochronology methods. This allows for a retroactive analysis of CO_2ff mole

20 fractions over many years, including any trends in emissions that occurred during the life of

21 the tree. The radiocarbon content in tree rings has been well established as a tracer for fossil

22 CO_2 emissions (Suess, 1955; Tans et al., 1979; Djuricin et al., 2012; Rakowski et al., 2013)

23 and as a method to detect leaks from CO_2 geosequestration (Donders et al., 2013).

24 In this study, we evaluate whether we can detect changes in CO_2ff emission rates from a point

25 source on an annual time scale using the CO_2ff mole fraction derived from the ^{14}C content of

26 tree ring archives. Variations in the observed CO_2ff mole fraction at a given location are

27 dependent on not only the emission rate but also on atmospheric transport, which in turn is

28 subject to naturally varying meteorological conditions (e.g. wind speed and direction,

29 temperature, pressure, etc.). Detecting a change in the emission rate requires disentangling

30 this change from the natural variability in transport and meteorology as well as from

31 measurement uncertainty in the observations. The question we ask in this paper is: can we use

32 tree ring archives to detect changes in CO_2ff emissions from a point source, and if so, what is

1 the minimum change in annual emissions that we can detect given the typical measurement
2 uncertainty of 1ppm and natural variability in transport? A similar analysis was carried out by
3 Levin and Rodenbeck (2007) at the regional scale, using a 20-year time series of [14]C
4 observations over Germany. McKain et al. (2012) also assessed the ability of an observation-
5 model framework to detect changes in regional urban CO_2 emissions on a monthly time scale.
6 We re-examine this question on the scale of an individual point source with mean annual
7 observations.

8 We calculate interannual variability in observations from tree ring archives of annual
9 (growing season) CO_2ff between 2004-05 and 2011-12[1], taken from two different trees
10 growing south of the Kapuni Natural Gas Treatment Plant in rural New Zealand (Norris,
11 2015). We then use an atmospheric transport model, WindTrax, with local meteorological
12 data to quantify the interannual variability that can be expected due to measurement
13 uncertainty, transport and meteorology at different distances and orientations from the source,
14 including the locations of the trees. Finally, we look at what this implies for detection limits in
15 the context of emissions monitoring or verification and practical considerations in the
16 presence of multiple sources of uncertainty.

18 **2   Methods**

19 **2.1   Site**

20 The site of our study is the Kapuni Natural Gas Treatment Plant in rural Taranaki, New
21 Zealand (39.477° S, 174.1725° E, 170 m.a.s.l.) (Fig. 1). This site was chosen because it is
22 located in flat terrain and is relatively isolated from other sources of CO_2ff, considerably
23 simplifying measurement and analysis. The gas treatment plant, owned and operated by
24 Vector, processes natural gas extracted from natural gas wells in the Taranaki Basin. The gas
25 contains around 40% CO_2, which is removed during processing and vented to the atmosphere
26 at a rate of ~0.1 TgC yr^{-1} (NZMED, 2010). In addition, there is an ammonia urea
27 manufacturing plant 500m to the west of the gas plant (Fig. 1a), operated by Ballance Agri-
28 Nutrients, which also releases CO_2ff to the atmosphere during the manufacturing process.
29 This site emits roughly a third of the amount of the Vector gas plant (~0.03 TgC yr^{-1})

---

[1] Henceforth in this paper, the growing season spanning 1 September to 30 April will be referred to by the year
in which the season began, i.e. 2004-05 will be designated 2004.

(Taranaki Regional Council, 2013). Although the signal from the Vector plant is much stronger, especially to the east (downwind from the dominant westerly winds), emissions from the Ballance plant are potentially large enough to detect at some locations and are included in our simulations unless otherwise specified.

The surrounding terrain is flat and mostly free of obstructions, with elevation varying no more than 10m within 2km of the plant. The largest nearby topographic feature is a dip of ~5m into the Kapuni stream immediately east of the Vector emission source. The landscape is dominated by highly productive pasture grazed by dairy cows, with large and diurnally varying CO_2 fluxes. The prevailing wind direction is from the west, with a smaller proportion from the southeast and north (Figs. 2 and 3).

2.2 CO_2 emissions

Emissions data were supplied by Vector as monthly totals (Peter Stephenson, personal communication), which we have converted to average daily rates for the purpose of modelling. Mean annual daily emissions for each year between 2004 and 2011 from 1 September to 30 April are shown in Fig. 4; data are listed in Table S1. The long-term mean is 5341 gC s^{-1}, with a standard deviation in annual means of 388 (7.3%). There are annual fluctuations but no long-term trend over the modelled period 2004-2011. The largest change during a single year occurred in 2007, when the emissions dropped by 14% relative to the mean. On a longer time scale, there are more significant changes, including the start of operations at the Vector Plant in 1971. However, we focus on the 2004-2011 period during which high resolution local meteorological data is available. There are no significant seasonal or diurnal variations in the emissions of which we are aware.

The Ballance Agri-Nutrients Plant emissions are reported on an annual basis (Taranaki Regional Council, 2013). Average daily rates in each growing season are depicted in Fig. 4. The mean daily rate of emissions over the period 2004-2011 is 1512 gC s^{-1} with a standard deviation in annual means of 88 (18%), which is more variable than the emissions from the Vector plant, but smaller in absolute terms. Emissions vary somewhat from day to day according to production levels, but more detailed daily or monthly information is unavailable; for simplicity we assume a constant emissions rate in each year. We note that emissions are much lower in 2011, which is due to downtime after both a fire and scheduled maintenance (Taranaki Regional Council, 2013).

2.3 Tree ring observations

Tree rings faithfully record the ^{14}C content of assimilated CO_2, so when the rings are independently dated by dendrochronology, we can determine an average ^{14}C content and recently added CO_2ff in the local atmosphere for the period during which the tree ring was laid down. We use core samples from two individual trees located south of the plant, one pine tree (*Pinus radiata*) and one chestnut tree (*Castanea sativa*) (Fig. 1a; Norris, 2015). The pine tree is located in a stand of trees within 5m of the Kapuni stream, with the crown reaching 10m above the associated terrain dip. The chestnut is isolated in a flat paddock.

Each tree ring is assumed to represent the Southern Hemisphere summer growth period from 1 September to 30 April, as this is when the majority of plant photosynthesis occurs and new plant material is produced. The sample preparation, measurement and determination of CO_2ff are described in detail by Norris (2015). In summary, wood was sampled from the trees using a Haglöff incremental borer. Four cores were extracted per tree at equidistant points at a height of approximately 1.2m from the base of the tree. One core from each tree was used to create a historic record of CO_2 emissions from commission of the Kapuni plant in 1971 to the outermost ring at the time of sampling in 2012. Replicates were taken from a second core to validate ring counting and ^{14}C results. Alpha cellulose was extracted from individual rings using a method modified from Hua et al. (2000), combusted with a Europa ANCA elemental analyser (EA), reduced to graphite and measured by accelerator mass spectrometry at GNS Science laboratories in Lower Hutt, New Zealand (Baisden et al., 2013; Zondervan et al., 2015; Turnbull et al., 2015).

CO_2ff was determined following Turnbull et al. (2014) from the isotopic difference between the measured tree ring and clean air background CO_2 measured at Baring Head, Wellington (41.4167°S, 174.8667°E; Currie et al., 2011; extended with unpublished data). Baring Head, located at the southern end of New Zealand's North Island and approximately 300 km south of Kapuni, was chosen as the background for this study over more local sites because it provides a long-term record of background CO_2 and ^{14}C, dating back to the early 1970s. The following equation was used:

$$C_{ff} = \frac{C_{obs}\left(\Delta_{obs} - \Delta_{bg}\right)}{\left(\Delta_{ff} - \Delta_{bg}\right)} - \beta \tag{1}$$

1   where C_{ff} is CO_2ff, C_{obs} is the CO_2 mole fraction in the observed sample, Δ_{obs} and Δ_{bg} are the

2    $\Delta^{14}C$ of the observed sample and background sample, respectively. Δ_{ff} is the $\Delta^{14}C$ of CO_2ff,

3   and is assigned to be -1000‰. Δ_{bg} is from the summer season average from the long-term

4   Wellington $^{14}CO_2$ record at Baring Head. Comparison of this record with tree rings collected

5   3 km upwind of our source showed no difference from the Wellington record. β is a small

6   correction to account for the fact that the $\Delta^{14}C$ of CO_2 from other sources may be slightly

7   different from that of the atmosphere; in our case we set β to zero since the proximity to the

8   coast and consistent winds suggest that CO_2other is negligible in this location (Turnbull et al.,

9   2014). Uncertainty in CO_2ff is dominated by $\Delta^{14}C$ measurement uncertainty in both

10   background and the observed sample and is typically ~1ppm for this dataset.

11   The process of CO_2 adsorption in plants is extremely complex. For simplicity, we assume a

12   constant assimilation rate over all daylight hours. In reality, CO_2 adsorption varies with plant

13   species and photosynthesis rates, being weighted towards sunny periods and midday

14   (Bozhinova et al., 2013). There are also many different climatic and nutrient limitations that

15   can only be properly accounted for with a full process-based biogeochemical model of plant

16   growth, which is beyond the scope of this study. We do, however, take into consideration the

17   fact that plant material will tend to underestimate mean CO_2ff when CO_2ff is variable, as in

18   the case of a plume from a point source (see Sect. 2.7).

19   **2.4 WindTrax model**

20   WindTrax (WindTrax 2.0; Thunder Beach Scientific, Nanaimo, Canada,

21   www.thunderbeachscientific.com) is a Lagrangian particle dispersion model used to estimate

22   unknown trace gas concentrations or emission rates from a source over short distances

23   (~1km). WindTrax has been applied to agricultural emissions from area sources, such as

24   methane, ammonia, and other gasses from grazing dairy cows, cattle feedlots and farm waste

25   (e.g. Flesch et al., 2005; Laubach and Kelliher, 2005; Bonifacio et al., 2013; Rhoades et al.,

26   2010; Wilson et al., 2012; McBain and Desjardins, 2005). It has also been assessed in the

27   context of CO_2 sequestration leakage detection (Leuning et al., 2008; Loh et al., 2009).

28   Modelling integrated averages of CO_2ff in plant material is a relatively new application.

29   WindTrax was chosen for this study because it is easy to use and the distance scale is

30   appropriate for our site. We previously used WindTrax to estimate CO_2ff in grass samples at

31   the Kapuni site (Turnbull et al., 2014), demonstrating that the model is capable of providing

32   reasonable estimates of observed CO_2ff. Here, we take the same approach to model CO_2ff

1 measured in tree rings. We note that WindTrax is not applicable to complex terrain or larger

2 distance scales and caution is urged when applying our methodology to other sites.

3 WindTrax simulates the transport of trace gases by releasing a set number of particles at each

4 time step and following each particle's trajectory downwind. Based on Monin–Obukhov

5 similarity theory (MOST), the physics underlying the model is described in detail in Flesch et

6 al. (2004) and Wilson and Sawford (1996). The model equations are valid in the atmospheric

7 surface layer. It assumes wind and other meteorological observations are averaged over a

8 suitable time interval representing a stable, mean atmospheric state (model relationships are

9 built from wind statistics over 15-60 minute intervals; using model time steps greatly outside

10 of this range is not recommended). Intervals longer than one hour can be problematic (Flesch

11 et al., 2004) because at these time intervals, large-scale fluctuations not described by MOST

12 statistics become important. In this study, we use one-hour time steps to match the resolution

13 of our meteorological dataset (see Sect. 2.5).

14 The model can be run in forward (fLS) or inverse/backward (bLS) mode, depending on

15 whether the emissions or the trace gas mole fractions are unknown. In all simulations

16 described here we start with known emission rates and use the fLS mode to estimate the

17 CO_2ff mole fraction at locations surrounding the plant. Model "concentration sensors"

18 represent simulated measurements of mole fractions at designated locations and supply the

19 main model output.

20 The model is stochastic, meaning that it introduces random turbulence into particle

21 trajectories, and no two runs are identical, even with the same parameters and meteorological

22 input. There is, therefore, inherent error in the model predictions due to the randomness

23 introduced in the transport process. Only the average behaviour of a group of particles can be

24 determined, and releasing more particles at each time step will tend to reduce the degree of

25 uncertainty. Statistical error (or the standard deviation within each set of trajectories) is

26 calculated and output by the model at each time step. However, any biases in the modelled

27 transport or the meteorological input data used to drive the model are not accounted for.

28 ## 2.5 Meteorology

29 Modelling with WindTrax requires at a minimum wind speed, wind direction, air temperature,

30 and atmospheric pressure at each time step. We use hourly meteorological data from the

31 Hawera Automatic Weather Station (AWS) (39.6117°S, 174.2917°E, 98 m.a.s.l), downloaded

from the New Zealand National Climate Database (CliFlo, 2014). Hawera, approximately 20km distance to the southwest of Kapuni, is the nearest location with a nearly complete long-term dataset of hourly wind direction and speed. Eight years of data (2004-2011) were available at the time of our study. We use only data from the growing season (1 September – 30 April) and daylight hours (08:00 – 18:00 local daylight savings time) in the model simulations to correspond to the time period during which trees assimilate CO_2. A wind rose for all eight growing seasons is shown in Fig. 2a.

The area to the northwest of Hawera and Kapuni is dominated by Mount Taranaki, a 2518m volcanic cone that rises steeply from relatively flat surrounding terrain. Wind direction and speed can be very different at sites only a few kilometres apart because of the local impact of the mountain on atmospheric flow. Thus we compared Hawera and Kapuni meteorological datasets to ensure that Hawera is representative of Kapuni over long (~1 year) time periods and the wind speed and direction distributions as a whole are similar at both locations. Daily mean wind speeds were compared using the Virtual Climate Station Network (VCSN; Tait et al., 2006). This is a set of "virtual" weather stations that uses re-analysis interpolation techniques to provide historical daily weather variables on a 5 x 5 km grid across New Zealand. The mean wind speed at Hawera over the modelled time period, 5.0 m s^{-1}, is only slightly higher than that at Kapuni, 4.6 m s^{-1}. Histograms comparing the wind speed distributions at both sites are in Fig. S1.

Only one overlapping dataset with sub-daily time intervals was available for direct comparison at the time of our study. We collected data at a temporary meteorological station situated in a paddock at Kapuni at 10-minute intervals during the period 14 August – 26 October 2012, with some data gaps (Turnbull et al., 2014). These were averaged to hourly intervals and compared with the corresponding set of measurements at the Hawera AWS. Only daylight hours were included for consistency with the model simulations. Wind roses for the Kapuni dataset and the corresponding time period at Hawera are shown in Figs. 2b and 2c. The distribution in direction is similar to the north, but there are more southerlies and fewer westerlies at Hawera. Using these datasets, correlation in wind speed is good, with $R^2 = 0.82$, and correlation in wind direction is moderate ($R^2 = 0.61$). Because wind direction is an angular measurement, correlation in wind direction was performed using the circular package v0.4-7 in R v3.0.2 (Lund and Agostinelli, 2013; R Core Team, 2013) rather than the standard linear correlation function. Scatter plots comparing wind speed and direction at Kapuni and

1   Hawera directly at each time step are in Fig. S2. Wind speed is a good match, with Hawera on

2   average having slightly higher speeds than Kapuni. When wind speed at Hawera is linearly

3   regressed against wind speed at Kapuni, the resulting equation is $y = 0.90x - 0.32$. (Model II

4   regression was performed with the lmodel2 v1.7-2 package in R v3.0.2 (Legendre, 2014)).

5   With wind direction, most points are close to the 1:1 line or slightly below, indicating a small

6   rotation in direction between the sites. Approximately 67% of data points (one sigma) are

7   within 30° of each other, and 85% are within 45°. For the purpose of our simulation in which

8   we focus on integrated averages rather than particular points in time, the Hawera dataset is

9   sufficiently representative of typical conditions at Kapuni. We note, however, that the dataset

10 from Kapuni spans a very limited time period, and this is a potential source of error in our

11 results.

12 We expect variability in CO_2ff mole fraction to be strongly related to variability in wind

13 speed and direction, and consequently sampling location. Annual mean wind speed does not

14 vary by much; the mean hourly wind speed over all eight years is 6.3 m s^{-1}, and the standard

15 deviation in annual mean is 0.11 m s^{-1}, which is only 2% of the mean. Mean wind direction is

16 273° (from the west), but there is also a significant amount of wind from the southeast and

17 north-northeast (Figs. 2 and 3). This general pattern did not change from year to year over the

18 eight years of the simulation, but relative proportions in each direction did sometimes vary

19 considerably (Fig. 3). In particular, northerlies (the direction most relevant to our

20 observations) range from 21-28% of the total, a 30% change in the northerly fraction. While

21 always the largest category, the percentage of westerlies varies between 38-52%. It is notable

22 that there are very few periods with calm winds; the region is in general very windy.

2.6 Model parameters

24 Several model parameters are held constant throughout all simulations. The modelled surface

25 is short grass (surface roughness z_o = 2.3cm), since the majority of the surrounding area is

26 grazed dairy pasture. The heights of the two emissions stacks are set to their known values:

27 35m above ground level for Vector and 36m for Ballance. The model's atmospheric stability

28 parameter is also held constant using the general class of 'moderately unstable'. While this is

29 not true for all modelled time periods, in the absence of measurements from a 3D sonic

30 anemometer or other reliable indicators of atmospheric stability, a general stability class is a

31 first approximation. We tested the model at a different constant stability class ('slightly

32 unstable') and found no significant difference in the amount of variability (results not shown).

1 We note, however, that atmospheric stability is a potential source of error; others have found

2 that stability is an important parameter that can bias results, and model estimates are generally

3 improved with input from a sonic anemometer or vertical profiles of wind speed and

4 temperature (Flesch et al., 2004; Gao et al., 2009; Koehn et al., 2013).

5 Model concentration sensors at the locations of the pine and chestnut trees are placed at

6 heights of 15.0m and 5.0m, respectively, reflecting the approximate height of the canopy. A

7 single height at each tree was chosen to reduce model complexity and runtime; however, we

8 recognize that in reality CO_2 is assimilated over a range of heights at each tree, corresponding

9 to the vertical spread of the canopy. Some previous studies have indicated that concentrations

10 modelled with WindTrax are sensitive to sampling height and/or the ratio of sampling height

11 to distance from the source (e.g. McBain and Desjardins, 2005; Laubach and Kelliher, 2005;

12 Laubach, 2010). To test for dependence on height, we simulated CO_2ff along a 20m vertical

13 profile at the location of the pine and chestnut trees (results not shown). Results vary

14 somewhat according to height, and averaging over a 5m height range slightly reduces the

15 mean and interannual standard deviation, but not enough to change our results significantly.

2.7 Simulations

17 We ran a "constant emissions, variable meteorology" simulation at an hourly time step with

18 all eight years of available meteorological data from Hawera (excluding night time and winter

19 months), concentration sensors placed at the locations of the trees, and both the Vector and

20 Ballance plants as CO_2ff point sources (Fig. 1). Because emissions are held constant, this

21 simulation enables us to isolate contributions to variability from meteorology and transport.

22 For each tree, four concentration sensors were placed on the vertices of a square, with sides of

23 length 30m, centred on the location of the trees and averaged to reduce model transport error.

24 The emission rate at each source was the reported mean rate over the entire modelled period.

25 In addition to the model sensors at the locations of the trees, we placed sensors at hypothetical

26 locations in four directions and two horizontal distances from the emissions source to

27 examine more general model sensitivity and variability due to meteorological conditions at

28 our site without being tied to the locations of specific observations. Eight additional sensors

29 were placed 1.5m above the ground in the four cardinal directions relative to the Vector plant,

30 one each at 300m and 600m horizontal distance from the source. Only one point source, the

1 Vector plant, was included in the results at these sensors to simplify analysis. Emissions are
2 constant at the Vector mean rate over the eight years.

3 We also ran a "constant meteorology, variable emissions" simulation in which we repeat the
4 meteorology from one year (2004) and allow emissions rates to vary according to the reported
5 values. This allows us to examine model annual variability due to emissions, independent of
6 transport.

7 We subsequently generated a "variable emissions, variable meteorology" simulation by
8 scaling modelled mole fractions at the tree rings from the constant emissions, variable
9 meteorology simulation according to reported emissions levels in each year (Fig. 4). This is
10 valid because the relationship between source strength and concentration flux passing through
11 a location downwind is linear (Leuning et al., 2008). In addition, under unstable atmospheric
12 conditions the emissions leave the model domain within one hour and do not return, so data in
13 a given year is not affected by the emissions from previous years. This simulation is used to
14 compare the model to observations.

15 Because plant material will underestimate mean CO_2ff when CO_2ff is variable, rather than
16 comparing the tree ring measurements to the raw model output of CO_2 mole fractions, we
17 calculate a modelled "CO_2ff_{tree}". This is the CO_2ff that the model would predict from the plant
18 material given measured background levels and the equations governing $\Delta^{14}C$. We use the
19 following equations:

$$20 \quad \Delta_i = \frac{\Delta_{bg} C_{bg} + \Delta_{ff} C_{ff\,i}}{C_{bg} + C_{ff\,i}} \tag{2}$$

$$21 \quad \Delta_{tree} = \frac{1}{N} \sum_{i=1}^{N} \Delta_i \tag{3}$$

$$22 \quad C_{ff\,tree} = \frac{C_{bg} (\Delta_{tree} - \Delta_{bg})}{\Delta_{ff} - \Delta_{tree}} \tag{4}$$

23 where $\Delta = \Delta^{14}C$, $C_{ff\,i}$ is the modelled CO_2ff at the ith time step, N is the total number of model
24 time time steps, C_{bg} and Δ_{bg} are measured (Norris, 2015), and Δ_{ff} = -1000. The basic
25 derivation of this equation can be found in Turnbull et al. (2006). This accounts for the fact
26 that plant material will assimilate roughly the same amount of CO_2 at each time step
27 regardless of the variability in atmospheric CO_2 mole fraction induced by the emission plume,
28 and thus the $\Delta^{14}C$ of the plant material represents a simple mean of the $\Delta^{14}C$ in the assimilated

CO_2 at each time step. In contrast, sampling of whole air across the same time period would collect more CO_2 during times of high CO_2 mole fraction, weighting the resultant $\Delta^{14}C$ towards these periods. This results in a CO_2ff_{tree} that is lower than would be obtained by determining the simple mean CO_2ff from the modelled mole fractions. Model results from the variable emissions simulation reported in Fig. 4 and Sect. 3 were derived using these equations.

3 Results and Discussion

3.1 Observation and model comparison

We first compare modelled CO_2ff_{tree} to the observed tree ring CO_2ff to evaluate the model's ability to estimate annual integrated averages in this context and to identify possible biases and error in the model. Our observations from tree rings consist of six annual measurements of CO_2ff from both the pine tree and the chestnut tree between 2004 and 2011 (2008 and 2010 are missing) (Fig. 4). The means over this period are 5.4ppm (pine) and 2.1ppm (chestnut) (Table 1). Mean modelled CO_2ff_{tree} over the same six years (excluding the two years without observations, 2008 and 2010) is 6.1ppm and 2.2ppm for the pine and chestnut tree, respectively. The modelled mean is almost an exact match for the chestnut tree (difference of 0.1ppm) and within error for the pine tree (difference of 0.7ppm). Figure 4 shows a direct comparison between measured and modelled CO_2ff for each year. At the pine tree, model performance is very good: four of the six (66%) annual observed values are within one sigma of the modelled values, and the remaining two are within two sigma. The agreement for individual years at the chestnut tree is poorer, but with large errors in the observations and the distance from the source close to the limit of model capabilities, this is expected.

The model is able to simulate both the long-term mean and the annual variation in CO_2ff_{tree} with a reasonable degree of accuracy, and there are no significant biases apparent. Thus we can be confident that the model is representative of relative interannual variability in transport, which is the focus for the remainder of this paper.

3.2 Drivers of interannual variability in CO_2ff

Detecting changes in emissions requires disentangling the changes in CO_2ff due to emissions from other sources of interannual variability. We now examine the variability in our

1   observations and turn to our model simulations to determine the relative contributions from

2   emissions, transport, and measurement uncertainty.

3   The observed standard deviations of the six annual CO_2ff values from the tree rings are

4   0.8ppm (14% of the six-year mean) and 1.1ppm (51%) for the pine and chestnut tree,

5   respectively (Table 1). This includes not only variability in emissions but other sources of

6   uncertainty such as meteorology and transport, variable ^{14}C assimilation rates in the trees,

7   precision of measurements, and background corrections. Measurement uncertainty in

8   particular is important at these relatively small concentrations. Given that the standard

9   deviations are very close to the typical measurement uncertainty of ~1ppm, the scatter in

10   annual means can be attributed in large part to this factor alone. For example, at the pine tree,

11   we would expect at least four out of six measurements to be within 1ppm (one sigma) of the

12   long-term mean, all other factors being constant. This is indeed true of four of the six

13   observations. Measurement uncertainty is proportionally much higher in the case of the

14   chestnut tree, which is ~1km from the Vector plant and where the average signal is only

15   ~2ppm. At this distance measurement uncertainty would seemingly dominate other sources of

16   variability. In contrast, the pine tree is much closer to the source (~400m), and the signal is

17   two to three times larger. Variations in emissions will make up a larger proportion of the total

18   variation and are more likely to be detectable at current measurement precision.

19   The standard deviations of modelled CO_2ff_{tree} in the variable emissions, variable meteorology

20   simulation are 0.5ppm (7.8%) and 0.3ppm (15%) at the pine and chestnut tree, respectively

21   (Table 1). Adding measurement uncertainty of 1ppm in quadrature, we would predict the

22   standard deviations of the annual means in observed CO_2ff to be 1.1ppm (18%) and 1.0ppm

23   (47%) for the pine and chestnut, respectively, if variability in emissions, atmospheric

24   transport and measurement uncertainty explain all of the interannual variability. In

25   comparison, the observed standard deviations of the annual means are 14% of the long-term

26   mean at the pine tree and 51% at the chestnut tree. Thus emissions, transport, and

27   measurement uncertainty are able to explain the interannual variability in the observations

28   within error.

29   We can estimate the relative proportion of interannual variability that is due to atmospheric

30   transport using the constant emissions model simulation, in which the only source of

31   variability is meteorology. The modelled mean CO_2ff over the six years with observations is

32   7.4ppm and 2.7ppm for the pine and chestnut, respectively, and modelled standard deviations

1   are both 0.5ppm (6.6% and 19% of the respective means) (Table 1). Over the full eight years

2   of the model simulation, the means and standard deviations are 7.7 / 0.9 ppm (12%) and 2.7 /

3   0.5 ppm (19%), respectively.

4   Examining more general patterns of meteorological and transport variability at the Kapuni site

5   apart from the locations of the trees reveals that the variation is highly dependent on the

6   direction of the observation location relative to the source. The results at the eight

7   hypothetical sensors averaged in each individual year and means for the entire eight years of

8   simulation are compared in Fig. 5, and the long-term means and standard deviations are given

9   in Table 2. The variation to the south of the plant (10-11% of the mean) is the lowest of any

10   direction and consistent with the variation found at the pine tree in the constant emissions

11   simulation over the full eight years (12%). Absolute CO_2ff mole fractions are highest in the

12   east (westerlies being dominant), but standard deviations are slightly higher at 14% of the

13   mean. Concentrations in the west are low (~2ppm) and highly variable, the result of the low

14   percentage of easterlies in any given year (Fig. 3). Variation is relatively insensitive to the

15   distance from the source.

16   It is apparent that wind direction drives a large part of the variation in transport. Annual

17   modelled CO_2ff at the trees in the constant emissions simulation is correlated with the annual

18   percentage of wind in the direction +/- 30° of the direct line between the source and the tree,

19   corresponding to the plume trajectories that are most likely to pass through the tree locations

20   (Fig. S3; R^2 = 0.56 and 0.72 for the pine and chestnut tree, respectively). The same correlation

21   between wind direction and modelled CO_2ff at all eight hypothetical sensors combined gives

22   an R^2 of 0.58. Over half of the transport variability is thus explained solely by variation in the

23   percentage of wind in each direction. However, other meteorological variables and model

24   parameters (e.g. wind speed, temperature, pressure, etc.) still play a non-negligible role, as the

25   annual variation in wind direction is not equivalent to the interannual variability in modelled

26   CO_2ff.

27   In the same manner, we can determine the contribution of changes in emission rates to the

28   overall interannual variability with the constant meteorology simulation in which emissions

29   vary but transport is the same in each year. This results in interannual variability in CO_2ff

30   similar to the variability in the emissions themselves, with the magnitude roughly scaled to

31   the distance from the emission source: the standard deviations are 0.5ppm (7.4%) and 0.2ppm

32   (7.6%) for the pine and chestnut tree, respectively. In comparison, the standard deviation of

the average daily emissions rate over the six years with observations is 7.9% of the mean for the Vector plant and 21% for the Ballance plant, with a standard deviation of 8.1% for the combined total (over the full eight years between 2004 and 2011, the standard deviations are 7.3% and 18% of the 8-year mean for Vector and Ballance emissions, respectively, and the variation in the combined emissions is 7.7%). This is on the same order of magnitude of the variability due to transport at the pine tree but only about half the amount at the chestnut tree.

Looking at all of the factors together (Table 1), variations in emissions and transport contribute about equally to total variation at the pine tree. At the chestnut tree, transport makes up a larger proportion of the total, which likely reflects the greater variability in meteorology in that particular direction. The variability in emissions somewhat counter-balances the variability in transport, particularly at the chestnut tree, where the standard deviation with both variable emissions and meteorology (0.3ppm / 15%) is lower than that with constant emissions (0.5ppm / 19%). This is most likely coincidental to the particular years of observations, as there is no correlation between variations in emissions and variations in transport (not shown). Meteorological variation happens to be lowest in the south, where the trees are located, even though the largest signal occurs to the east (Table 2 and Fig. 5). In this respect, the trees are fortuitously located for our study. This underscores the benefit of analysing transport variability at a particular location before collecting observations, as the quality of results can be greatly influenced by meteorological patterns.

3.3 Detection limits

Given the amount of interannual variation in meteorology and transport that we can infer from the model and typical measurement uncertainty of 1ppm, what is the minimum change in emissions that it is possible to detect in a tree ring sample taken at Kapuni, representing an integrated average of CO_2ff over a year or more? We use a student t-test to quantify the minimum amount of change in observations required (relative to the long-term average or reference period) that would allow us to conclude that there has been a change in emissions. The t-test calculates the minimum difference between the long-term mean and a new annual tree ring sample (or samples) that would be statistically significant above scatter or noise from other factors. We make the assumption that our observations and simulated mole fractions are normally distributed. The results of the 2-sided test (representing change in either direction) at a 95% confidence level are given in Table 3 for "future" samples representing one, two and four years of integrated average CO_2ff. All percentages are relative to the long-term mean

1 over six years, our reference period for this study. We assume that the standard deviation in

2 future samples due to interannual variability in meteorology is the same as the standard

3 deviation over the reference period.

4 Using the modelled means and standard deviations from the constant emissions simulation of

5 tree ring CO_2ff and measurement uncertainty of 1.0ppm, the detection limits represent the

6 minimum observed change that would indicate a driver of variability other than transport or

7 measurement uncertainty, in this case CO_2ff emissions. With a new observation representing

8 one year (i.e. one tree ring), the difference between the long-term mean and the new sample

9 would need to be more than 42% at the pine tree and 115% at the chestnut tree to have high

10 confidence that the sample shows a change in emissions, rather than just natural variability or

11 uncertainty. If we have four new annual observations at the new emission rate, the difference

12 reduces by half to 22% and 62%, respectively. These detection thresholds are well above the

13 reported annual changes in emission rates between 2004 and 2011 (Fig. 4). At the distance

14 and location of the chestnut tree (~1km), it seems likely that the signal is too small and

15 variable to be practical for detecting emission changes for a point source with emissions of

16 this magnitude.

17 If we relax the condition to one sigma (or a 68% confidence level), would we be able to detect

18 the largest change in emissions reported at the Vector Plant between 2004 and 2011? The

19 student t-test at 68% confidence level gives corresponding detection limits listed in Table 3.

20 For a one-year observation from the pine tree, this is 18%; for the chestnut, it is 92%. The

21 largest change in emissions in any single year at the Vector plant is in 2007, with a decline of

22 14% relative to the long-term mean, still below the detection limit. Indeed, looking at the

23 results in Fig. 4, the decline (0.4ppm, or 19% of the mean) at the chestnut tree in 2007 is not

24 significant; there is also a small decline (0.7ppm, or 13% of the mean) in CO_2ff at the pine

25 tree but it is again too small to conclude that emissions have changed. If we were able to

26 achieve a reduction in measurement uncertainty to 0.5ppm, however, the threshold for

27 detection at the pine tree becomes an 11% change in emissions, and we would expect to be

28 able to observe a 14% decline in emissions. In this case, the small decline in CO_2ff at the pine

29 tree in 2007 would be significant.

30 Would we be able to detect this change at a different location (in direction and/or distance)

31 around the Kapuni plant? Our hypothetical concentration sensors 300m and 600m from the

32 source (Table 2) indicate that with a single one-year CO_2ff observation, only a change in

emissions of at least 36% would be detectable at 95% confidence, a much larger change than occurs in our observational dataset. The location of the pine tree (at 400m southeast of the plant) appears to provide as good a detection capability as any of our hypothetical sensors. However, if we have four years of observations (and the change in emissions was sustained over that time period) located either to the east or the south of the plant at a distance of 300m, we would be able to detect a change of 10% or more at the one-sigma confidence level. Changes of 20% or more would be detectable at these same locations with one year of observations, or alternately, four years of observations if we require high confidence.

This analysis uses the actual meteorology only to determine the interannual variability in CO_2ff that we might expect due to meteorological variations. If we also know the meteorology in the year or years of the new observations, we can quantify the change in emissions by modelling transport at constant emissions. For example, attributing 15% of the one-year variation at the pine tree to the combined factors of transport and measurement uncertainty (Table 1) and assuming that the rest of the variation is due to emissions, this translates to a change in emissions of 27% over the one year. In this manner it is possible to get a more precise estimate of the long-term changes in emissions.

Additionally, if we have multiple measurements over the same period at different locations around the point source, measurement uncertainty reduces proportionally by $1/\sqrt{n}$, where n is the number of independent measurements. The resulting reduction in detection thresholds is more complex and depends on the long-term mean and variation at each of the observation locations. One could, for example, use a paired t-test to determine if the change detected in all of the measurements taken together is significant. This is beyond the scope of the current study, but the detection thresholds given in Tables 2 and 3, based on a single observation location, would overestimate the minimum change in emissions that it is possible to observe with multiple measurements designed to cover the area surrounding the point source.

3.4 Applicability to other point sources

The results presented here are specific to the meteorology and point sources at the Kapuni site, but the methodology can be extended to any point source with suitable trees growing nearby. Ideally, observations would be made as close to the source as possible in the direction where the signal is strongest and/or most consistent. If measurement uncertainty of 1ppm is to be relatively unimportant compared to the combined transport and emissions variability of 8%

at the pine tree (i.e. adding measurement uncertainty does not change the total variation in measured CO_2ff by more than 1-2%), we require a signal around 20-30ppm, implying a required emission rate five times that of the Kapuni Vector plant. Alternatively, if we were able to reduce measurement uncertainty to 0.5ppm (for example, by increased measurement precision or taking measurements from multiple locations at the site), we would be able to detect changes with signals at around half the magnitude, and the method could be more feasible for emission sources the size of the Kapuni Vector Plant. Additionally, if we have multiple measurements from the same period at various locations surrounding the source, detection thresholds lower further and we can achieve the same sensitivity with a smaller point source.

Our case study involves point sources that are fairly small on an international scale; for comparison, the world's largest power plant, in Taiwan, emits about 300,000 gC s^{-1} or 9.5 TgC yr^{-1} (Ummel, 2012), which is 95 times as much as the Vector plant at Kapuni. There are approximately 800 power plants worldwide that emit more than 10 times the annual total CO_2ff at Kapuni (CARMAv3.0, 2009; Wheeler and Ummel, 2008; Ummel, 2012). The typical emission rates seen at these larger power plants would produce signals in which measurement uncertainty is only a small proportion of the total. With annual signals theoretically 10 times that observed at the Kapuni pine tree and the same amount of meteorological variation, all other things being equal, the detection threshold for a one-year measurement at the location of the pine tree would be 19%, or 10% with four years of measurements. This is a plausible reduction target, and the method would be useful for verifying emissions changes in such cases.

The Kapuni site has several advantages that simplify the modelling component of this method: the terrain is flat, and there are trees conveniently located close to the CO_2ff sources. With larger distance scales and/or more complex terrain, WindTrax might not be an appropriate choice of model. Alternative atmospheric transport models that are applicable to larger distances (hundreds of kilometres and/or regional scales) and more complicated geographic features include CALPUFF (Scire et al., 2000), WRF-CHEM (Grell et al., 2005), and AERMOD (Cimorelli et al., 2005). While these models would need to be tested in the context of our method, the same general principles would apply.

4 Conclusions

We have examined sources of interannual variability in CO_2ff in samples from tree ring archives representing integrated averages over one year. We used the atmospheric transport model WindTrax to separate variability in meteorology and transport from other sources of variation in our observations. At the location of the pine tree, modelled variation in transport is 7% of the six-year reference mean. This is about the same magnitude as the variation in emissions that were recorded over the same time period. At the chestnut tree, variation due to atmospheric transport is larger, at 19% of the mean, and is about twice the magnitude of the variation in emissions. Taking into account typical measurement uncertainty of 1ppm for radiocarbon samples, in order to conclude with high confidence that there has been a change in emissions and not just natural variation in meteorology, we would require an observed change of 42% from the mean in a new one-year sample from the pine tree. If we take a two-year or four-year sample average, this reduces to 30% and 22%, respectively. This is well above the largest single-year change in emissions at the Vector Plant, which is 14%. However, if we are able to reduce measurement uncertainty by half, to 0.5ppm, or if the point source doubles in strength, detection thresholds are closer to the actual level of variation in emissions. If we only require confidence at the one-sigma level, we would in this case be able to detect a 14% change in a single year.

Detection limits are highly dependent on the location of the observations and specific meteorology of the site. Wind patterns should be carefully considered before deciding where to take samples in any study, preferably in an area where the signal will be strongest and where wind patterns will be most consistent through time. A model analysis such as we have performed can give an idea of the baseline variability in transport and the size of the signal needed to observe changes in emissions. This makes it theoretically possible to separate the uncertainty in transport from other sources of uncertainty.

In general, this method will be most effective when observations are made in the dominant wind direction and/or in a direction with consistent winds, close enough to the point source so that natural variability in meteorological conditions and measurement uncertainty does not overwhelm the signal from the emissions. The larger the point source (the higher the emission rate) and the signal from CO_2ff, the more able integrated averages from plant material will be to detect changes in emissions. For larger power plants or other point sources of a more typical size worldwide, detecting changes with this method could be feasible; with signals 10

times or more the size of Kapuni, measurement uncertainty is relatively insignificant, and sustained changes in emissions on the order of 10% can be detected from a single sampling location given suitable meteorological conditions and observations.

Acknowledgements

This work was funded by GNS Science Strategic Development Fund and public research funding from the Government of New Zealand. Marcus Trimble assisted with sample collection, dendrochronology and sample preparation. The Rafter Radiocarbon Laboratory staff (Jenny Dahl, Johannes Kaiser, Kelly Lyons, Christine Prior, Helen Zhang and Albert Zondervan) were invaluable in their assistance with the radiocarbon measurements. We thank Peter Stephenson and the staff at the Vector Kapuni Gas Processing Plant for providing information on the plant's CO_2 emissions and allowing us to sample trees on their site. We also thank Roger Luscombe for allowing access to his land and chestnut tree for sampling and his extensive knowledge of local history. Finally, thank you to two anonymous referees whose comments have improved this manuscript.

References

Ackerman, K. V., and Sundquist, E. T.: Comparison of two US power-plant carbon dioxide emissions data sets, Environ. Sci. Technol., 42, 5688-5693, 2008.

Baisden,,W. T., Prior, C. A., Chambers, D., Canessa, S., Phillips, A., Bertrand, C., Zondervan, A., and Turnbull, J. C.: Radiocarbon sample preparation and data flow at Rafter: accommodating enhanced throughput and precision, Nucl. Instrum. Meth. B, 294, 194–198, 2013.

Boden, T. A., Marland, G., and Andres, R. J.: Global, Regional, and National Fossil-Fuel CO_2 Emissions, Carbon Dioxide Information Analysis Center, Oak Ridge National Laboratory, U.S. Department of Energy, Oak Ridge, Tenn., USA, doi 10.3334/CDIAC/00001_V2015, 2015.

Bonifacio, H. F., Maghirang, R. G., Razote, E. B., Trabue, S. L., and Prueger, J. H.: Comparison of AERMOD and WindTrax dispersion models in determining PM10 emission rates from a beef cattle feedlot, J. Air Waste Manage., 63, 545-556, 2013.

Bozhinova, D., Combe, M., Palstra, S. W. L., Meijer, H. A. J., Krol, M. C., and Peters, W.: The importance of crop growth modeling to interpret the $\Delta^{14}CO_2$ signature of annual plants, Global Biogeochem. Cy., 27, 792-803, 2013.

Brioude, J., Angevine, W. M., Ahmadov, R., Kim, S.-W., Evan, S., McKeen, S. A., Hsie, E.-Y., Frost, G. J., Neuman, J. A., Pollack, I. B., Peischl, J., Ryerson, T. B., Holloway, J., Brown, S. S., Nowak, J. B., Roberts, J. M., Wofsy, S. C., Santoni, G. W., Oda, T., and Trainer, M.: Top-down estimate of surface flux in the Los Angeles Basin using a mesoscale inverse modeling technique: assessing anthropogenic emissions of CO, NO_x and CO_2 and their impacts, Atmos. Chem. Phys., 13, 3661-3677, doi:10.5194/acp-13-3661-2013, 2013.

Cimorelli, A. J., Perry, S. G., Venkatram, A., Weil, J. C., Paine, R. J., Wilson, R. B., Lee, R. F., Peters, W. D., and Brode, R. W.: AERMOD: A Dispersion Model for Industrial Source Applications. Part I: General Model Formulation and Boundary Layer Characterization, J. Appl. Meteor., 44, 682–693, doi: http://dx.doi.org/10.1175/JAM2227.1, 2005.

CliFlo: NIWA's National Climate Database on the Web: http://cliflo.niwa.co.nz/ , last access: 4 November 2014.

Currie, K. I., Brailsford, G., Nichol, S., Gomez, A., Sparks, R., Lassey, K. R., and Riedel, K.: Tropospheric $^{14}CO_2$ at Wellington, New Zealand: the world's longest record, Biogeochemistry, 104, 5-22, 2011.

Djuricin. S., Xu. X., and Pataki, D.E.: The radiocarbon composition of tree rings as a tracer of local fossil fuel emissions in the Los Angeles basin: 1980-2008, J. Geophys. Res-Atmos., 117, D12303, 2012.

Donders, T. H., Decuyper, M., Beaubien, S. E., van Hoof, T. B., Cherubini, P., and Sass-Klaassen, U.: Tree rings as biosensor to detect leakage of subsurface fossil CO_2. Int. J. Greenh. Gas Con., 19, 387-395, 2013.

eGRID: Technical Support Document for the 9th Edition of eGRID with Year 2010 Data (Emissions & Generation Resource Integrated Database), Washington, D.C., 2014.

Flesch, T. K., Wilson, J. D., Harper, L., Crenna, B., and Sharpe, R.: Deducing ground-to-air emissions from observed trace gas concentrations: a field trial, J. Appl. Meteorol., 43, 487–502, 2004.

Flesch, T. K., Wilson, J. D., Harper, L., and Crenna, B: Estimating gas emissions from a farm with an inverse-dispersion technique, Atmos. Envir., 39, 4863–4874, 2005.

Gao, Z., Mauder, M., Desjardins, R. L., Flesch, T. K., and van Haarlem, R. P.: Assessment of the backward Lagrangian stochastic dispersion technique for continuous measurements of CH_4 emissions, Agr. Forest Meteorol., 149, 1516-1523, 2009.

Geels, C., Gloor, M., Ciais, P., Bousquet, P., Peylin, P., Vermeulen, A. T., Dargaville, R., Aalto, T., Brandt, J., Christensen, J. H., Frohn, L. M., Haszpra, L., Karstens, U., Rödenbeck, C., Ramonet, M., Carboni, G., and Santaguida, R.: Comparing atmospheric transport models for future regional inversions over Europe – Part 1: mapping the atmospheric CO_2 signals, Atmos. Chem. Phys., 7, 3461-3479, doi:10.5194/acp-7-3461-2007, 2007.

Gerbig, C., Körner, S., and Lin, J. C.: Vertical mixing in atmospheric tracer transport models: error characterization and propagation, Atmos. Chem. Phys., 8, 591-602, doi:10.5194/acp-8-591-2008, 2008.

Grell, G. A., Peckham, S. E., Schmitz, R., McKeen, S. A., Frost, G., Skamarock, W. C., and Eder, B.: Fully coupled "online" chemistry within the WRF model, Atmos. Environ., 39, 6957-6975, 2000.

Gurney, K. R.: Beyond Hammers and Nails: Mitigating and Verifying Greenhouse Gas Emissions, Eos Trans. AGU, 94, 199, 2013.

Gurney, K. R., Mendoza, D. L., Zhou, Y., Fischer, M. L., Miller, C. C., Geethakumar, S., and de la Rue du Can, S.: High resolution fossil fuel combustion CO_2 emission fluxes for the United States, Environ. Sci. Technol., 43, 5535-5541, 2009.

Gurney, K. R., Razlivanov, I., Song, Y., Zhou, Y., Benes, B., and Abdul-Massih, M.: Quantification of fossil fuel CO_2 emissions on the building/street scale for a large US City, Environ. Sci. Technol., 46, 12194-12202, 2012.

Hua, Q., Barbetti, M., Jacobsen, G.E., Zoppi, U. and Lawson, E.M.: Bomb radiocarbon in annual tree rings from Thailand and Australia, Nucl. Instrum. Meth. B, 172, 359-365, 2000.

IPCC Core Writing Team, Pachauri, R. K. and Meyer, L. A. (Eds.): Climate Change 2014: Synthesis Report. Contribution of Working Groups I, II and III to the Fifth Assessment Report of the Intergovernmental Panel on Climate Change, IPCC, Geneva, Switzerland, 151 pp., 2014.

Karlen, I., Olsson, I. U., Kllburg, P., and Kilici, S.: Absolute determination of the activity of two ^{14}C dating standards, Arkiv Geofysik, 4, 465–471, 1968.

Koehn, A. C., Leytem, A. B., and Bjorneberg, D. L.: Comparison of atmospheric stability methods for calculating ammonia and methane emission rates with WindTrax, Transactions of the American Society of Agricultural and Biological Engineers, 56, 763-768, 2013.

Kretschmer, R., Gerbig, C., Karstens, U., and Koch, F.-T.: Error characterization of CO_2 vertical mixing in the atmospheric transport model WRF-VPRM, Atmos. Chem. Phys., 12, 2441-2458, doi:10.5194/acp-12-2441-2012, 2012.

Laubach, J.: Testing of a Lagrangian model of dispersion in the surface layer with cattle methane emissions, Agr. Forest Meteorol., 150, 1428-1442, 2010.

Laubach, J., and Kelliher, F. M.: Methane emissions from dairy cows: Comparing open-path laser measurements to profile-based techniques, Agr. Forest Meteorol., 135, 340-345, 2005.

Legendre, P.: lmodel2: Model II Regression, R package version 1.7-2, available at: http://CRAN.R-project.org/package=lmodel2, published: 24 February 2014.

Leuning, R., Etheridge, D., Luhar, A., and Dunse, B.: Atmospheric monitoring and verification technologies for CO_2 geosequestration, Int. J. Greenh. Gas Con., 2, 401-414, 2008.

Levin, I., and Rödenbeck, C.: Can the envisaged reductions of fossil fuel CO_2 emissions be detected by atmospheric observations?, Naturwissenschaften, 95, 203-208, doi:10.1007/s00114-007-0313-4, 2007.

Levin, I., Kromer, B., Schmidt, M., and Sartorius, H.: A novel approach for independent budgeting of fossil fuel CO_2 over Europe by $^{14}CO_2$ observations, Geophys. Res. Lett., 30, 2194, doi:10.1029/2003GL018477, 2003.

Lin, J. C., and Gerbig, C.: Accounting for the effect of transport errors on tracer inversions, Geophys. Res. Lett., 32, L01802, doi:10.1029/2004GL021127, 2005.

Lindenmaier, R., Dubey, M. K., Henderson, B. G., Butterfield, Z.T., Herman, J. R., Rahn, T., and Lee, S. H.: Multiscale observations of CO_2, $^{13}CO_2$, and pollutants at Four Corners for emission verification and attribution, P. Natl. Acad. Sci. USA, 111, 8386-8391, 2014.

Liu, J., Fung, I., Kalnay, E., and Kang, J.-S.: CO_2 transport uncertainties from the uncertainties in meteorological fields, Geophys. Res. Lett., 38, L12808, doi:10.1029/2011GL047213, 2011.

Loh, Z., Leuning, R., Zegelin, S., Etheridge, D., Bai, M., Naylor, T., and Griffith, D.: Testing Lagrangian atmospheric dispersion modelling to monitor CO_2 and CH_4 leakage from geosequestration, Atmos. Environ., 43, 2602–2611, doi:10.1016/j.atmosenv.2009.01.053, 2009.

Lund, U., and Agostinelli, C.: circular: Circular Statistics, R package version 0.4-7, available at: http://cran.r-project.org/web/packages/circular/index.html (last access: 29 Jan 2015), 2013.

McBain, M. C., and Desjardins, R. L.: The evaluation of a backward Lagrangian stochastic (bLS) model to estimate greenhouse gas emissions from agricultural sources using a synthetic tracer source, Agr. Forest Meteorol., 135, 61-72, 2005.

McKain, K., Wofsy, S. C., Nehrkorn, T., Eluszkiewicz, J., Ehleringer, J. R., and Stephens, B. B.: Assessment of ground-based atmospheric observations for verification of greenhouse gas emissions from an urban region, P. Natl. Acad. Sci. USA, 109, 8423-8428, 2012.

1 Meijer, H. A. J., Smid, H. M., Perez, E., and Keizer, M. G.: Isotopic characterisation of
2 anthropogenic CO_2 emissions using isotopic and radiocarbon analysis, Phys. Chem. Earth, 21,
3 483-487, 1996.

4 Miles, N. L., Richardson, S. J., Davis, K. J., Lauvaux, T., Andrews, A. E., West, T., Bandaru,
5 V., and Crosson, E. R.: Large amplitude spatial and temporal gradients in atmospheric
6 boundary layer CO_2 mole fractions detected with a tower-based network in the US Upper
7 Midwest, J. Geophys. Res., 117, G01019, 2012.

8 National Research Council: Verifying Greenhouse Gas Emissions: Methods to Support
9 International Climate Agreements, The National Academies Press, Washington, D.C., USA,
10 124 pp., 2010.

11 Nisbet, E., and Weiss, R.: Top-down versus bottom-up, Science, 328, 1241-1243, 2010.

12 Norris, M. W.: Reconstruction of historic fossil CO_2 emissions using radiocarbon
13 measurements from tree rings, M.S. thesis, Victoria University of Wellington, Wellington,
14 New Zealand, 155 pp., 2015.

15 NZMED: New Zealand's Energy Outlook 2010, New Zealand Ministry of Economic
16 Development, Wellington, New Zealand, 12 pp., 2010.

17 Prather, M. J., Zhu, X., Strahan, S. E., Steenrod, S. D., and Rodriguez, J. M.: Quantifying
18 errors in trace species transport modeling, P. Natl. Acad. Sci. USA, 105, 19617-19621, 2008.

19 R Core Team: R: A language and environment for statistical computing, R Foundation for
20 Statistical Computing, Vienna, Austria, available at: http://www.R-project.org/ (last access:
21 21 August 2014), 2013.

22 Rakowski, A. Z., Nadeau, M. J., Nakamura, T., Pazdur, A., Pawełczyk, S., and Piotrowska,
23 N.: Radiocarbon method in environmental monitoring of CO_2 emission, Nucl. Instrum. Meth.
24 B, 294, 503-507, 2013.

25 Rhoades, M. B., Parker, D. B., Cole, N. A., Todd, R. W., Caraway, E. A., Auvermann, B. W.,
26 Topliff, D.R. and Schuster, G. L.: Continuous ammonia emission measurements from a
27 commercial beef feedyard in Texas, Transactions of the American Society of Agricultural and
28 Biological Engineers, 53, 1823-1831, 2010.

29 Scire, J. S., Strimaitis, D. G., and Yamartino, R. J.: A user's guide for the CALPUFF
30 dispersion model, Earth Tech, Inc, Concord, Massachusetts, USA, 2000.

Serre, C., Santikarn, M., Stelmakh, K., Eden, A., Frerk, M., Kachi, A., Unger, C., Wilkening, K., and Haug, C. (Eds): Emissions Trading Worldwide: International Carbon Action Partnership (ICAP) Status Report 2015, International Carbon Action Partnership, Berlin, Germany, 71 pp., 2015.

Stephens, B. B., Gurney, K. R., Tans, P. P., Sweeney, C., Peters, W., Bruhwiler, L., Ciais, P., Ramonet, M., Bousquet, P., Nakazawa, T., Aoki, S., Machida, T., Inoue, G., Vinnichenko, N., Lloyd, J., Jordan, A., Heimann, M., Shibistova, O., Langenfelds, R. L., Steele, L. P., Francey, R. J., Denning, A. S.: Weak Northern and Strong Tropical Land Carbon Uptake from Vertical Profiles of Atmospheric CO_2, Science, 316, 1732-1735, 2007.

Suess, H. E.: Radiocarbon concentration in modern wood, Science, 122, 415, 1955.

Tait, A., Henderson, R., Turner, R., and Zheng, X. G.: Thin plate smoothing spline interpolation of daily rainfall for New Zealand using a climatological rainfall surface, Int. J. Climatol., 26, 2097-2115, 2006.

Tans, P. P., and Wallace, D. W.: Carbon cycle research after Kyoto, Tellus B, 51, 562-571, 1999.

Tans, P. P., De Jong, A. F. M., and Mook, W. G.: Natural atmospheric ^{14}C variation and the Suess effect, Nature, 280, 826-828, 1979.

Taranaki Regional Council: Ballance Agri-Nutrients (Kapuni) Ltd Monitoring Programme Biennial Report 2010-2012: Technical Report 2012-91, Taranaki Regional Council, Stratford, New Zealand, 63 pp., June 2013.

Turnbull, J. C., Miller, J. B., Lehman, S. J., Tans, P. P., Sparks, R. J., and Southon, J. R.: Comparison of $^{14}CO_2$, CO and SF_6 as tracers for determination of recently added fossil fuel CO_2 in the atmosphere and implications for biological CO_2 exchange, Geophys. Res. Lett., 33, L01817, doi:10.1029/2005GL024213, 2006.

Turnbull, J. C., Keller, E. D., Baisden, W. T., Brailsford, G., Bromley, T., Norris, M. W., and Zondervan, A.: Atmospheric measurement of point source fossil fuel CO_2 emissions, Atmos. Chem. Phys., 14, 50001-5014, doi: 10.5194/acp-14-5001-2014, 2014.

Ummel, K.: CARMA revisited: an updated database of carbon dioxide emissions from power plants worldwide, Center for Global Development Working Paper 304, Center for Global Development, Washington, D.C., USA, 2012.

1   United Nations Framework Convention on Climate Change (UNFCCC): Kyoto Protocol,

2   available at: http://unfccc.int/kyoto_protocol/items/2830.php, and Intended Nationally

3   Determined Contributions, available at: http://unfccc.int/focus/indc_portal/items/8766.php

4   (last access: 29 May 2015), 2015.

5   U.S. Environmental Protection Agency: Plain English Guide to the Part 75 Rule, U.S.

6   Environmental Protection Agency, Washington, D.C., USA, 118 pp., 2005.

7   Wheeler, D., and Ummel, K.: Calculating CARMA: global estimation of CO_2 emissions from

8   the power sector, Center for Global Development Working Paper 145, Center for Global

9   Development, Washington, D.C., USA, 2008.

10   Wilson, J. D., and Sawford, B. L.: Review of Lagrangian stochastic models for trajectories in

11   the turbulent atmosphere, Bound.-Lay. Meteorol., 78, 191–210, 1996.

12   Wilson, J. D., Flesch, T. K., and Crenna, B. P.: Estimating Surface-Air Gas Fluxes by Inverse

13   Dispersion Using a Backward Lagrangian Stochastic Trajectory Model, in: Lagrangian

14   Modeling of the Atmosphere, Lin, J., Brunner, D., Gerbig, C., Stohl, A., Luhar, A., and

15   Webley, P. (Eds.), American Geophysical Union, Washington, D. C., USA, doi:

16   10.1029/2012GM001269, 2012.

17   Zondervan, A., Hauser, T.M., Kaiser, J., Kitchen, R.L., Turnbull, J.C. and West, J.G.:

18   XCAMS: The compact 14 C accelerator mass spectrometer extended for 10 Be and 26 Al at

19   GNS Science, New Zealand, Nucl. Instrum. Meth. B, 361, 25-33, 2015.

1 Table 1. Observed and modelled CO_2ff means and standard deviations at the locations of the
2 pine and chestnut tree between 2004 and 2011. All means and standard deviations (SD)
3 include six years (2008 and 2010 are omitted because there are no observations available for
4 these years). Measurement uncertainty (MU) of 1.0ppm is explicitly added to the modelled
5 results in the far right column. Observations implicitly include this uncertainty.

Observation or simulation (2004-2011)	Mean (ppm)	SD (% of mean)	SD + 1.0ppm MU (% of mean)
Pine			
Observed	5.4		0.8 (14%)
Modelled CO_2ff_{tree} : variable meteorology, variable emissions	6.1	0.5 (7.8%)	1.1 (18%)
Modelled CO_2ff : variable meteorology, constant emissions	7.4	0.5 (6.6%)	1.1 (15%)
Modelled CO_2ff : constant meteorology, variable emissions	7.3	0.5 (7.4%)	1.1 (15%)
Chestnut			
Observed	2.1		1.1 (51%)
Modelled CO_2ff_{tree} : variable meteorology, variable emissions	2.2	0.3 (15%)	1.0 (47%)
Modelled CO_2ff : variable meteorology, constant emissions	2.7	0.5 (19%)	1.1 (41%)
Modelled CO_2ff : constant meteorology, variable emissions	2.3	0.2 (7.6%)	1.0 (43%)

1 Table 2. Modelled mean CO_2ff and standard deviation (SD) of eight hypothetical sensors

2 simulated over the eight years 2004-2011 with constant emissions. Measurement uncertainty

3 (MU) of 1.0ppm is added to the standard deviation in the fourth column. Columns 5-10 show

4 the detection limits calculated at the two-sigma (95%) and one-sigma (68%) confidence level

5 (CL) for samples representing an average of one, two, or four years. Measurement uncertainty

6 (MU) of 1.0ppm is added in quadrature to the standard deviation of modelled CO_2ff before

7 limits are calculated.

Model Sensor	Mean (ppm)	SD (% of mean)	SD + 1ppm MU (% of mean)	% change detectable (95% CL)			% change detectable (68% CL)		
				1 yr	2 yr	4 yr	1 yr	2 yr	4 yr
North 300m	12.2	2.4 (20%)	2.6 (21%)	53%	38%	29%	24%	18%	13%
North 600m	4.6	0.8 (18%)	1.3 (29%)	72%	52%	39%	33%	24%	18%
East 300m	22.8	3.2 (14%)	3.3 (15%)	37%	27%	20%	17%	12%	9.4%
East 600m	9.0	1.3 (14%)	1.6 (18%)	45%	33%	24%	20%	15%	12%
South 300m	11.7	1.3 (11%)	1.7 (14%)	36%	26%	20%	16%	12%	9.2%
South 600m	4.7	0.5 (10%)	1.1 (24%)	60%	43%	33%	27%	20%	15%
West 300m	1.6	0.8 (50%)	1.3 (81%)	204%	148%	111%	92%	68%	52%
West 600m	0.34	0.16 (50%)	1.0 (300%)	744%	540%	405%	337%	250%	190%

Table 3. Detection limits for samples at the pine and chestnut trees, calculated with modelled CO_2ff at constant emissions and six years of observations in reference period (2004-2011). Limits are given at the two-sigma (95%) and one-sigma (68%) confidence level (CL) for samples representing an average of one, two, or four years. Measurement uncertainty (MU) of 1.0ppm or 0.5ppm is added in quadrature to the standard deviation of modelled CO_2ff before limits are calculated.

Modelled CO_2ff: variable meteorology constant emissions	% change detectable (95% CL)			% change detectable (68% CL)		
	1 yr	2 yr	4yr	1 yr	2 yr	4yr
Pine						
Modelled CO_2ff + 1.0 MU	42%	30%	22%	18%	13%	10%
Modelled CO_2ff + 0.5 MU	27%	19%	14%	11%	8.5%	6.5%
Chestnut						
Modelled CO_2ff + 1.0 MU	115%	83%	62%	92%	68%	52%
Modelled CO_2ff + 0.5 MU	89%	64%	48%	38%	28%	22%
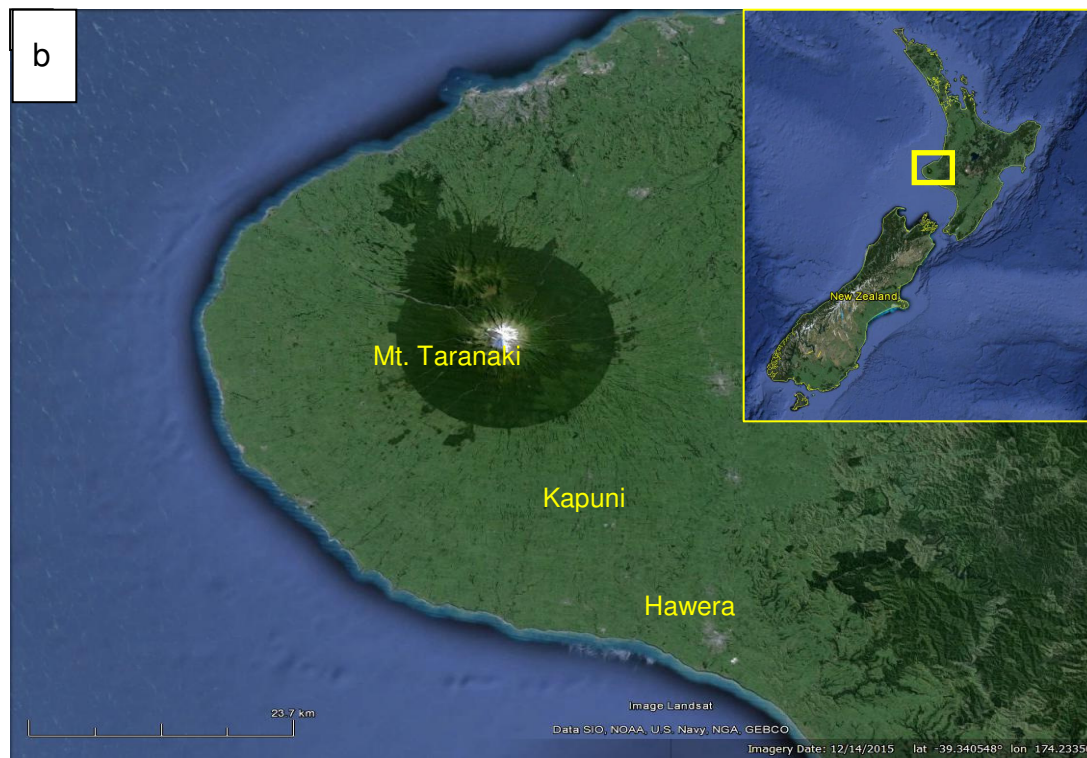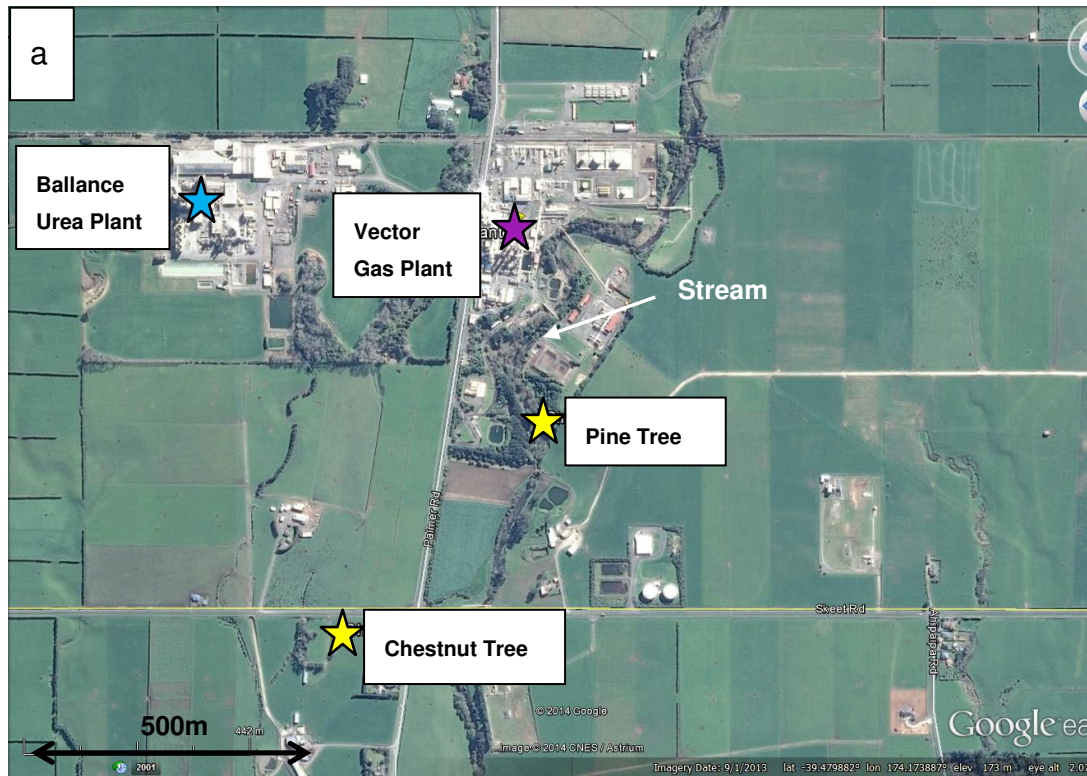
Figure 1. a) Aerial view of Kapuni area, with the sampled pine and chestnut trees, Kapuni Stream, and Vector Gas Treatment Plant and Ballance Agri-Nutrient Urea Plant labelled. b)

1   The Taranaki region, with Mount Taranaki, Kapuni, and Hawera labelled. Inset: New

2   Zealand, with the Taranaki region outlined in yellow
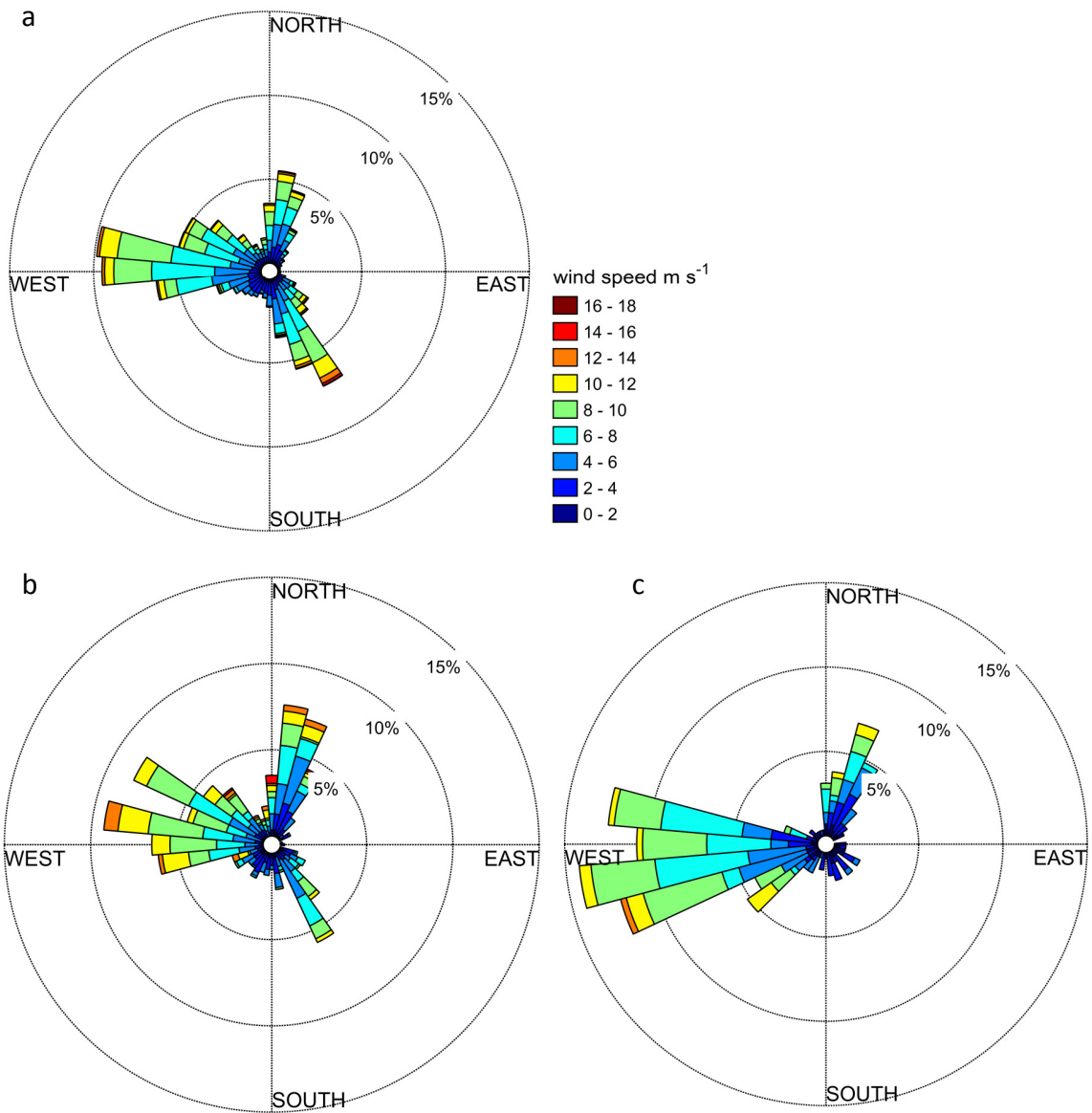
Figure 2. Wind roses at hourly intervals a) at Hawera during the eight growing season (Sep-Apr) between 2004-2011, b) Hawera 14 Aug – 26 Oct 2012, and c) Kapuni 14 Aug – 26 Oct 2012, all showing daylight hours only (8:00am – 6:00pm). Wind speed is in m s^{-1}. Data at Kapuni was collected at 10-minute intervals and averaged to hourly intervals to match Hawera data.
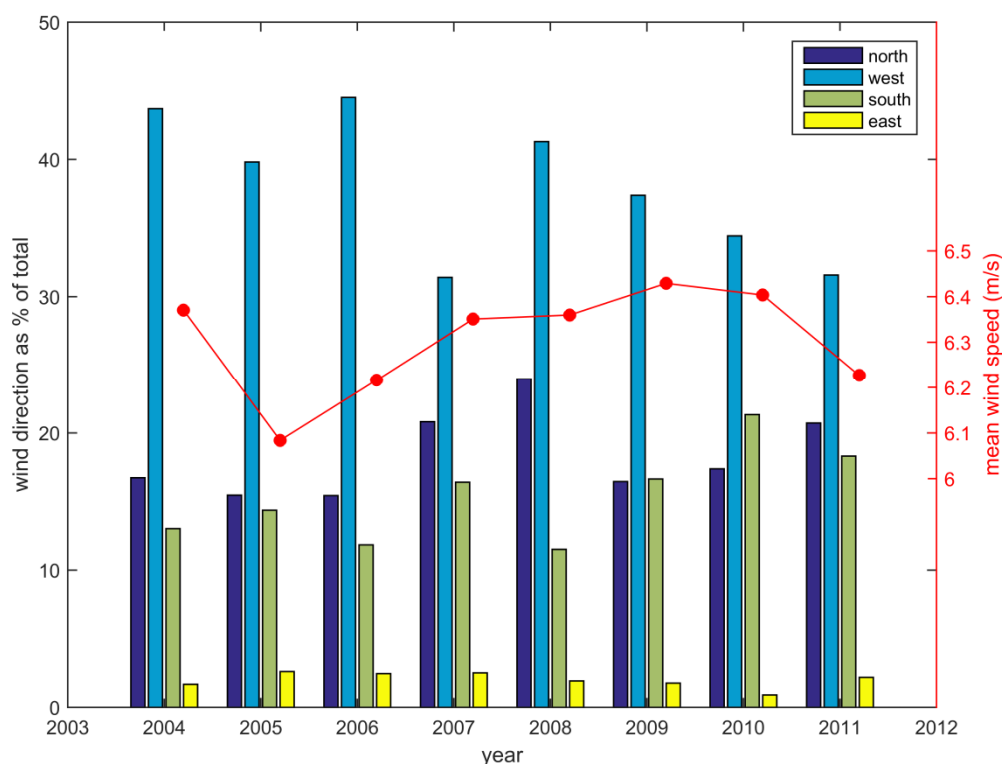
3 Figure 3. Percentage of wind measured at Hawera in each of four directions (left y-axis) and

4 mean wind speed (right y-axis) in each growing season (Sep-Apr) between 2004 and 2011

5 (daylight hours only, 8:00am – 6:00pm). Directions are defined by +/- 30 degrees due north,

6 west, south, and east (i.e. west is defined as wind from 240° to 300°). Note that this does not

7 comprise the complete 360° circle so percentages do not add to 100.
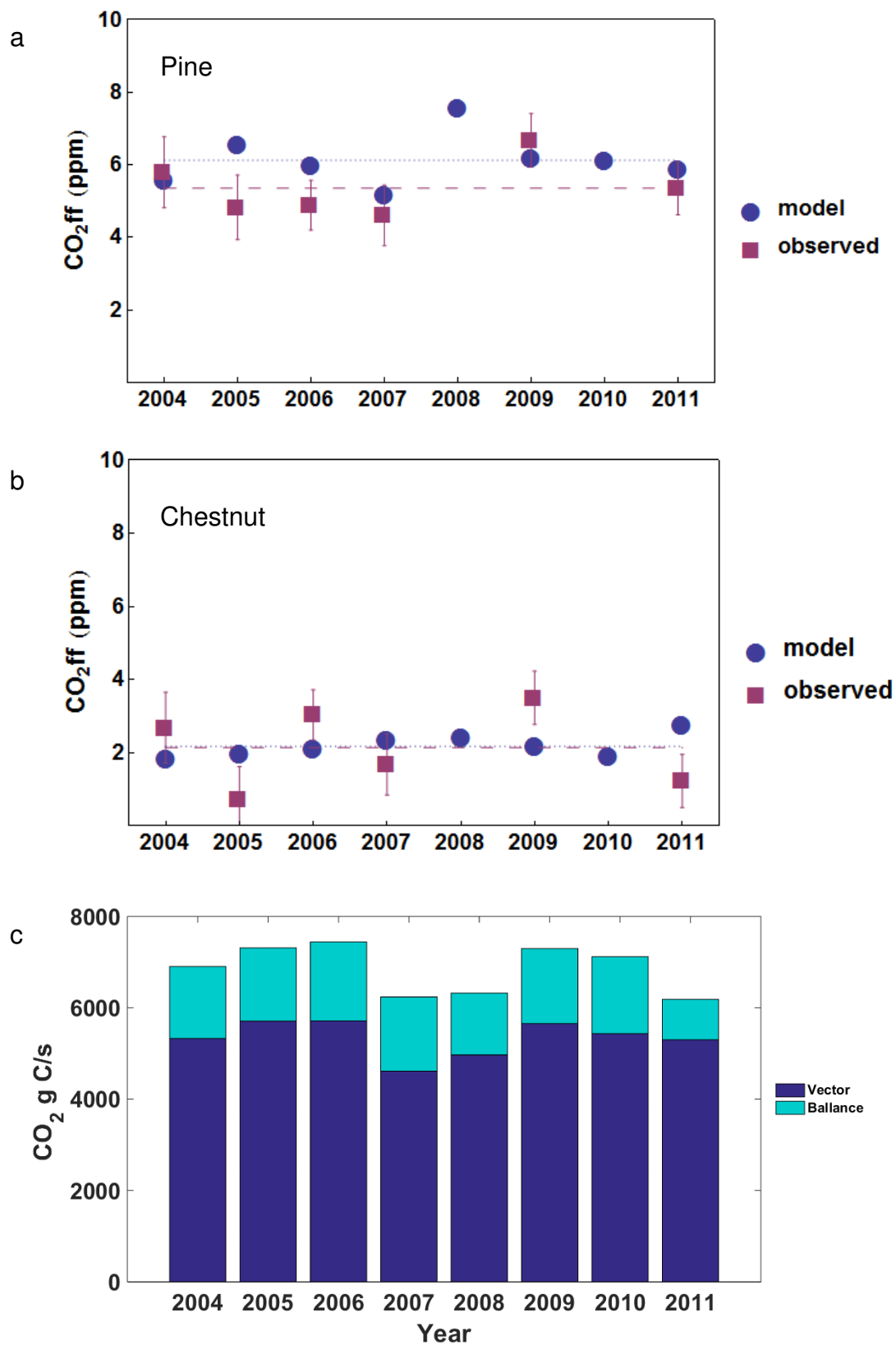
1   Figure 4. Pine tree (a) and chestnut tree (b) modelled CO_2ff_{tree} vs. observed CO_2ff in each year

2   between 2004 and 2011. Dotted and dashed lines show modelled and observed six-year

3   means, respectively (2008 and 2010 are excluded due to lack of observations). Bottom panel

4   (c) shows the average emissions rate in g C/s for Vector and Ballance in each year for

5   comparison.
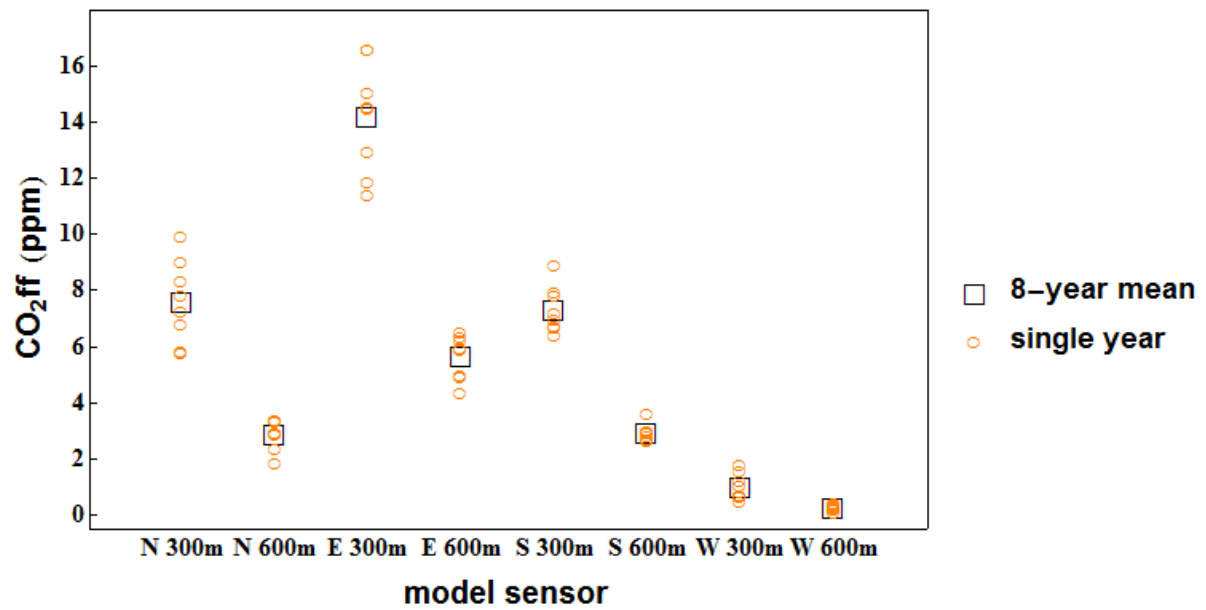
3 Figure 5. Constant emissions, variable meteorology simulation results for hypothetical

4 sensors: CO_2ff mole fraction averaged over all eight years of simulation (squares) and

5 individual annual averages (circles). Sensors are labelled on the x-axis by direction (N, E, S or

6 W) and distance (300m or 600m) from the source.